1521-009X/51/8/1024–1034$35.00
DRUG METABOLISM AND DISPOSITION

dx.doi.org/10.1124/dmd.123.001268
Drug Metab Dispos 51:1024–1034, August 2023

METTL7A (TMT1A) and METTL7B (TMT1B) Are Responsible for Alkyl *S*-Thiol Methyl Transferase Activity in Liver[S]

Drake A. Russell, Marvin K. Chau, Yuanyuan Shi, Ian N. Levasseur, Benjamin J. Maldonato, and Rheem A. Totah

University of Washington, Department of Medicinal Chemistry, Seattle, Washington

Received January 24, 2023; accepted April 27, 2023

ABSTRACT

S-methylation of drugs containing thiol-moieties often alters their activity and results in detoxification. Historically, scientists attributed methylation of exogenous aliphatic and phenolic thiols to a putative *S*-adenosyl-L-methionine (SAM)-dependent membrane-associated enzyme referred to as thiol methyltransferase (TMT). This putative TMT appeared to have a broad substrate specificity and methylated the thiol metabolite of spironolactone, mertansine, ziprasidone, captopril, and the active metabolites of the thienopyridine prodrugs, clopidogrel, and prasugrel. Despite TMT's role in the *S*-methylation of clinically relevant drugs, the enzyme(s) responsible for this activity remained unknown. We recently identified methyltransferase-like protein 7B (METTL7B) as an alkyl thiol methyltransferase. METTL7B is an endoplasmic reticulum–associated protein with similar biochemical properties and substrate specificity to the putative TMT. Yet, the historic TMT inhibitor 2,3-dichloro-α-methylbenzylamine (DCMB) did not inhibit METTL7B, indicating that multiple enzymes contribute to TMT activity. Here we report that methyltransferase-like protein 7A (METTL7A), an uncharacterized member of the METTL7 family, is also a SAM-dependent thiol methyltransferase. METTL7A exhibits similar biochemical properties to METTL7B and putative TMT, including inhibition by DCMB (IC_{50} = 1.17 μM). Applying quantitative proteomics to human liver microsomes and gene modulation experiments in HepG2 and HeLa cells, we determined that TMT activity correlates closely with METTL7A and METTL7B protein levels. Furthermore, purification of a novel His-GST–tagged recombinant protein and subsequent activity experiments prove that METTL7A can selectively methylate exogenous thiol-containing substrates, including 7α-thiospironolactone, dithiothreitol, 4-chlorothiophenol, and mertansine. We conclude that the METTL7 family encodes for two enzymes, METTL7A and METTL7B, which are now renamed thiol methyltransferase 1A (TMT1A) and thiol methyltransferase 1B (TMT1B), respectively, that are responsible for thiol methylation activity in human liver microsomes.

SIGNIFICANCE STATEMENT

We identified methyltransferase-like protein 7A (thiol methyltransferase 1A) and methyltransferase-like protein 7B (thiol methyltransferase 1B) as the enzymes responsible for the microsomal alkyl thiol methyltransferase (TMT) activity. These are the first two enzymes directly associated with microsomal TMT activity. *S*-methylation of commonly prescribed thiol-containing drugs alters their pharmacological activity and/or toxicity, and identifying the enzymes responsible for this activity will improve our understanding of the drug metabolism and pharmacokinetic (DMPK) properties of alkyl- or phenolic thiol–containing therapeutics.

Introduction

In humans, two distinct enzyme systems are associated with *S*-methyltransferase activity, thiopurine methyltransferase (TPMT) and a putative thiol methyltransferase (TMT) (Bremer and Greenberg, 1961; Yates et al., 1997). TPMT is a well characterized cytosolic enzyme, whereas putative TMT, or TMT activity, is used in the literature to describe one or more microsomal enzymes capable of thiol methylation, but the exact gene and protein remain uncharacterized. Both TPMT and TMT transfer a methyl group from the cofactor *S*-adenosyl-L-methionine (SAM) to a thiol group. Thiols are reactive nucleophiles capable of altering the oxidation potential of essential biomolecules by forming covalent bonds. TPMT is a well characterized methyltransferase that specifically methylates exogenous thiopurines (Krynetski and Evans, 2003), but to date no endogenous substrate has been identified. TPMT substrates such as 6-mercaptopurine and azathioprine belong to a class of immunosuppressive chemotherapeutic drugs with a narrow therapeutic index, and *S*-methylation is an inactivation and detoxification pathway. Genetic polymorphisms in TPMT, resulting in decreased methylation activity, often lead to toxicity from these drugs (Krynetski and Evans, 2003; Wusk et al., 2004). Weinshilboum et al. (Weinshilboum and Sladek, 1980) identified the enzyme responsible for TPMT activity in 1980, and many studies detailing the biochemical and

This work was supported in part by National Institutes of Health National Institute of General Medical Sciences [Grant T32-GM007750] (to D.A.R. and B.J.M.) and National Heart, Lung, and Blood Institute [Grant R01-HL146603].

No author has an actual or perceived conflict of interest with the contents of this article.

dx.doi.org/10.1124/dmd.123.001268.

[S] This article has supplemental material available at dmd.aspetjournals.org.

ABBREVIATIONS: CHAPS, 3-((3-cholamidopropyl)dimethylammonio)-1-propanesulfonate; DCMB, 2,3-dichloro-α-methylbenzylamine; DMPG, 1,2-dimyristoyl-sn-glycero-3-PG; DTT, dithiothreitol; EMEM, Eagle's minimum essential media; GSTrap FF, GSTrap Fast Flow; HLM, human liver microsome; K_i, inhibitor constant; K_m, Michealis constant; KPi, potassium phosphate; LC/MS, liquid chromatography–mass spectrometry; LC-MS/MS, liquid chromatography tandem mass spectrometry; METTL7A, methyltransferase-like protein 7A; METTL7B, methyltransferase-like protein 7B; SAH, *S*-adenosyl-homocysteine; SAM, *S*-adenosyl-L-methionine; siRNA, small interfering RNA; TMSL, 7α-thiomethylspironolactone; TMSL-D7, 7α-thiomethylspironolactone-d7 deuterated internal standard; TMT, thiol methyltransferase; TPMT, thiopurine methyltransferase; TSL, 7α-thiospironolactone.

structural characterization of TPMT have since followed. Today, patients are routinely screened for TPMT polymorphisms prior to thiopurine drug therapy (Lennard, 2014). In contrast, the enzyme(s) responsible for TMT activity were not known and as a result, historically, the microsomal fractions of various tissue homogenates were used to characterize TMT activity. Past research established that the enzyme(s) responsible for TMT activity do not share substrates with TPMT but are responsible for the SAM-dependent *S*-methylation of exogenous alkyl and phenolic thiol-containing compounds. Endogenous thiols such as glutathione and cysteine are not substrates for TMT.

Many drugs characterized as substrates for this putative TMT require their thiol functional group for activity, and methylation can dramatically alter their pharmacology. Potential substrates include 7α-thiospironolactone (TSL), mertansine, the active metabolites of prasugrel and clopidogrel, ziprasidone, and captopril (Keith et al., 1984; Erickson et al., 2010; Obach et al., 2012; Kazui et al., 2014; Liu et al., 2015; Taplin et al., 2018). In most cases, it is difficult to determine *a priori* how methylation changes the activity of a particular drug. For example, the *S*-methyl metabolite of spironolactone, 7α-thiomethylspironolactone (TMSL), is the major circulating metabolite and is responsible for most of the drug's activity in vivo (Overdiek and Merkus, 1987). Mertansine, a potent microtubule inhibitor that is conjugated to antibodies through a disulfide bond, contains a free thiol upon reduction and release from the attached antibody (Bargh et al., 2019). Interestingly, one report suggested that *S*-methylation of mertansine's free thiol alters its interaction with microtubules by increasing mertansine's effect on the dynamic instability of microtubules and promoting their aggregation, a mechanism of action that is quite distinct from the parent free thiol, which inhibits microtubule polymerization (Lopus et al., 2010). Clopidogrel and prasugrel are thienopyridine prodrugs that require activation via cytochrome P450–mediated ring opening to expose a reactive thiol that forms a disulfide bond with and irreversibly inhibits P_2Y_{12}, a transmembrane receptor that controls platelet aggregation (Savi et al., 2006). *S*-methylation of the reactive thiol results in the inactivation of these agents due to their inability to covalently bind to their receptor (Savi et al., 2006). A better characterization of the enzyme(s) responsible for TMT activity could provide clinicians and drug developers alike much needed insight when faced with a compound with an alkyl thiol.

Recently, we identified methyltransferase-like protein 7B (METTL7B) as an enzyme capable of catalyzing SAM-dependent methylation of alkyl thiols (Maldonato et al., 2021). METTL7B is a 28-kDa microsomal protein with similar tissue distribution and substrate specificity to the putative TMT (Zehmer et al., 2008). Although there is no specific inhibitor for the enzyme(s) responsible for TMT activity, 2,3-dichloro-α-methylbenzylamine (DCMB) potently inhibits TMT but not TPMT activity in liver microsomes (Glauser et al., 1993; Maw et al., 2018). Interestingly, despite possessing several attributes that are characteristic of an enzyme responsible for TMT activity, METTL7B is not inhibited by DCMB even at high concentrations, suggesting that additional enzymes may also account for microsomal TMT activity.

The gene known as *putative methyltransferase-like protein 7A* (*METTL7A*) codes for the protein METTL7A in the same family as METTL7B (Zehmer et al., 2008). METTL7A is predicted to be a membrane-associated methyltransferase and shares 75% sequence homology with METTL7B, but biochemical characterization that defines METTL7A's function is scant. In this work, we report that METTL7A, like METTL7B, is a SAM-dependent *S*-methyltransferase with many similarities to the historic TMT, including potent inhibition by DCMB. Using multiple approaches, including quantitative proteomics, single donor human liver microsomes (HLMs), and gene modulation experiments in HepG2 and HeLa cells, we determine that TMT activity is strongly associated with METTL7A protein levels. Furthermore, the purification of a novel His-GST–tagged recombinant protein and extensive biochemical characterization established that METTL7A methylates a wide variety of thiol-containing substrates, including TSL, dithiothreitol (DTT), 4-chlorothiophenol, and mertansine.

Materials and Methods

Chemicals, Materials, and Reagents. Activity assay substrates, reagents, cofactor, inhibitor, and internal standards: phenylethanolamine, dopamine, cysteine, 4-chlorothiophenol, and L-penicillamine were obtained from Sigma-Aldrich (St. Louis, MO); mertansine and 1,2-dimyristoyl-sn-glycero-3-PG (DMPG) were obtained from Cayman Chemicals (Ann Arbor, MI); 7α-thiospironolactone was produced in house from spironolactone using a previously published method (Agusti et al., 2013); spironolactone, reduced glutathione, captopril, and dithiothreitol were obtained from Fisher Scientific (Hampton, NH); *S*-methyl mertansine and 7α-thiomethylspironolactone-d7 (TMSL-D7) were obtained from Toronto Research Chemicals (Toronto, ON, Canada); *S*-adenosyl-L-methionine was obtained from New England Biolabs (Ipswich, MA); and 2,3-dichloro-α-methylbenzylamine was sourced from Enamine (Monmouth Junction, NJ). Reagents and materials for *Escherichia coli* culture, protein purification, and activity assay experiments: ampicillin sodium salt, isopropyl β-D-1-thiogalactopyranoside (IPTG), yeast extract, tryptone, NaCl, KH_2PO_4, K_2HPO_4, Thermo Scientific Halt Protease Inhibitor Cocktail, glycerol, 3-((3-cholamidopropyl)dimethylammonio)-1-propanesulfonate (CHAPS), white 96-well microplate, Nunc 96-Well Polypropylene Storage Microplates, Nunc 96-Well Slit-Cap Mats, and ultra-15 10K molecular weight cutoff centrifugal filter units were obtained from Fisher Scientific; His60 Ni Superflow Resin was obtained from Takara (Mountain View, CA); 5 ml GSTrap Fast Flow (GSTrap FF) column was obtained from Cytiva (Marlborough, MA); deoxyribonuclease I, lysozyme, and imidazole were obtained from Sigma-Aldrich; and MTase-Glo Methyltransferase Assay Kit was obtained from Promega (Madison, WI). All primers that are described for the sequencing or production of the N-GST METTL7A plasmid were obtained from Integrated DNA Technologies (San Diego, CA). Reagents and materials for activity assay cleanup and downstream liquid chromatography–mass spectrometry (LC/MS) analysis: acetonitrile (LC/MS grade), formic acid (LC/MS grade), acetic acid (LC/MS grade), Optima water, barium hydroxide, and zinc sulfate were obtained from Fisher Scientific; maleimide was obtained from Sigma-Aldrich. Reagents and materials for SDS-page and western blot analysis: NuPAGE MOPS SDS Running Buffer (20×), PageRuler Plus Prestained Protein Ladder (10 to 250 kDa), GelCode Blue Safe Protein Stain, iBlot Nitrocellulose Transfer Stacks, and METTL7B Rabbit Anti-Human Polyclonal Antibody were sourced from Fisher Scientific; Polyclonal Rabbit Anti-Human METTL7A Antibody was obtained from LifeSpan BioSciences (Seattle, WA); DYKDDDDK (Anti-FLAG) Tag Rabbit monoclonal antibody, β-actin rabbit monoclonal antibody, and GST-Tag rabbit monoclonal antibody were obtained from Cell Signaling (Danvers, MA); IRDye 680RD Goat Anti-Rabbit secondary antibody was obtained from LI-COR (Lincoln, NE); and Rabbit Polyclonal Anti-METTL7A Antibody was obtained from OriGene (Rockville, MD). Reagents and materials for cell culture and gene modulation: Eagle's Minimum Essential Medium, Gibco Opti-MEM, Gibco Penicillin-Streptomycin, Corning Falcon Polystyrene 12-well and 6-well Microplates, Gibco Trypsin-EDTA (0.25%), Cytiva HyClone Fetal Bovine Serum, Invitrogen Lipofectamine 3000 & P3000 Transfection Reagents, and cell culture–treated T75 plates were obtained from Fisher Scientific; Empty-, METTL7A-, and METTL7B-pCMV6 expression vectors were sourced from OriGene; Dulbecco′s Phosphate Buffered Saline (DPBS), METTL7A-specific small interfering RNA (siRNA), METTL7B-specific siRNA, and scramble nonspecific negative control siRNA were obtained from Sigma-Aldrich. Reagents for gene expression analysis: Invitrogen MagMAX Total RNA Isolation Kit, Applied Biosystems High-Capacity RNA-to-cDNA Kit, Applied Biosystems TaqMan Fast Advanced Master Mix, and reverse-transcription polymerase chain reaction (RT-PCR) primers specific for METTL7A, METTL7B, and GUSB were obtained from Fisher Scientific.

METTL7A Expression and Purification. Recombinant wild-type METTL7A (N-GST-METTL7A) was cloned in *E. coli* using a unique expression plasmid that was created in house. The expression plasmid backbone (pET21-

10XHis-GST-HRV-dL5) was a gift from Marcel Bruchez (Addgene plasmid # 73214; https://n2t.net/addgene:73214; RRID: Addgene_73214). An open reading frame sequence that codes for METTL7A (UniProt: Q9H8H3) was synthesized by Blue Heron Biotech (Bothell, WA) and inserted into the plasmid using BamHI and EcoRI restriction sites and general molecular biology techniques. The forward primer for insertion of the METTL7A sequence is as follows: 5′-CTAGCTAGGGATCCGCTCCGGCACCGGCTCCGGCACCGGCACCGATGGAGTTGACTATCTTCATCTTGCGCCTG-3′. The reverse primer for insertion of the METTL7A sequence was 5′-CTAGCTAGGAATTCTTATTAACGCGTTTTGACCGCGTA-3′. All plasmid inserts were validated by sequencing through Eurofins Genomics (Louisville, KY), and the sequencing histograms were analyzed using FinchTV software. The forward sequencing primer was 5′-GGGCTGGCAAGCCACGTTTGGTG-3′, and the reverse sequencing primer was 5′-CGTACCACTTCCACAAGTAAGTA-3′. The final expression plasmids positioned an N-terminal His-GST affinity tag onto the wild-type METTL7A protein sequence separated by a 10-residue poly-alanine-proline (AP)5 linker.

Expression plasmids were propagated using heat-shocked Stellar cells (Ref: 636763, Lot: 2106487A; Takara). Competent LOBSTR-BL21(DE3) *E. coli* (Ref: EC1002; Kerafast, Winston-Salem, NC) transformed via heat shock with plasmids validated by sequencing. *E. coli* cells were cultured in an orbital shaker at 250 rpm, 37°C, and in the presence of 100 μg/ml ampicillin.

To express recombinant protein in LOBSTR-BL21(DE3) cells, overnight cultures were added to ampicillin-containing terrific broth (TB) expression media at a ratio of 1:100. METTL7A production was initiated via the addition of isopropyl β-D-1-thiogalactopyranoside (IPTG) to a final concentration of 1 mM. The temperature was reduced to 15°C, and the cells were grown for an additional 24 hours. Cells were harvested via centrifugation at 2500 relative centrifugal force (RCF) for 30 minutes, and the resulting pellets were stored at −80°C until future processing.

Frozen cell pellets were thawed on ice in a 4°C cold cabinet overnight prior to resuspension in lysis buffer (50 mM potassium phosphate (KPi) pH 7.0, 20% glycerol, 150 mM NaCl, 10 mM CHAPS, EDTA-free Halt Protease Inhibitor Cocktail) supplemented with 100 μg/ml lysozyme (Ref: L-6876, Lot: 65H7025; Sigma-Aldrich). The lysate was placed on a rocker at 4°C until it became extremely viscous, and then 100 μg/ml DNA Nuclease I (Ref: DN25-100MG, Lot: SLCB6648; Sigma-Aldrich) was added and the lysate was placed on a rocker at 4°C until it was no longer viscous. The lysate was then centrifuged at 48,000 × *g* for 30 minutes at 4°C, and the resulting supernatant was retained for subsequent purification steps.

The purification was performed using a vertical column hand packed with 4 ml of His60 Ni Superflow Resin, followed by GST column purification using the ÄKTA start chromatography system (GE Healthcare, Chicago, IL). Cell lysate supernatant was added to the column containing nickel resin, and it was recirculated across the column by a peristaltic pump overnight at 0.5 ml/min. The column was washed with 50 column volumes of His60 Ni purification buffer (50 mM KPi pH 7.0, 20% glycerol, 10 mM CHAPS, 300 mM NaCl) containing 50 mM imidazole. The protein was eluted from the column with 10 column volumes of His60 Ni purification buffer containing 300 mM imidazole.

The His60 Ni-column eluent was directly applied to a preconditioned GSTrap FF column at a flow rate of 1 ml/min and recirculated for 4 hours. The column was then washed with GSTrap FF purification buffer (50 mM KPi pH 7.0, 20% glycerol, 10 mM CHAPS, 150 mM NaCl) until the absorbance at 280 nm decreased to baseline. The recombinant protein was eluted from the column using GSTrap FF purification buffer, which contained 10 mM reduced glutathione and was adjusted to pH 8.0. The eluent was concentrated using MilliporeSigma Amicon Ultra-15 10K molecular weight cutoff centrifugal filter units, and the final protein concentration was determined by A280 measurement. Purified protein stocks were aliquoted and stored at −80°C for future use.

Protein Purity Analysis. All SDS-PAGE Coomassie stained or western blot analysis was conducted with Invitrogen NuPAGE 4 to 12%, Bis-Tris, 1.0 mm, Mini Protein Gels in the XCell SureLock Mini-Cell Electrophoresis system using PageRuler Plus Prestained Protein Ladder as a molecular weight marker. Gels were run at room temperature and a constant 200 V. Total protein purity was determined with GelCode Blue Stain Reagent, a colloidal Coomassie dye. For western blot analysis, proteins were transferred to nitrocellulose membranes using the iBlot Gel Transfer Device. Primary antibody incubations were conducted overnight at 4°C at a 1:500 dilution with rabbit anti-METTL7A (Ref: LS-C82875, Lot: 178089; LifeSpan BioSciences), anti-METTL7B (Ref: PA5-58478, Lot: XC3518324A; Invitrogen, Carlsbad, CA), or anti-GST (#2625S, Lot:8; Cell Signaling) primary antibodies. The secondary incubation was performed at room temperature for 1 hour with IRDye 680RD goat anti-rabbit secondary antibody at a 1:10,000 dilution (Ref: 926-68071, Lot: D11102-15; LI-COR). Western blots and Coomassie-stained gels were visualized with an Odyssey gel scanner, and blot images were analyzed using Image Studio Version 4.0 software.

In Vitro 7α-Thiospironolactone and Captopril Methylation Using Recombinant METTL7A and METTL7B. For methyl transferase activity assays, aliquots of purified recombinant METTL7A or METTL7B were diluted with reaction buffer (50 mM KPi pH 7.0, 20% glycerol, 150 mM NaCl, 10 mM CHAPS) to 0.2 mg/ml. The diluted protein was then combined with two parts reaction buffer containing 9 mg/ml DMPG. A fraction of diluted protein was boiled for 10 minutes while the remaining active protein was incubated on ice for 30 minutes to equilibrate with DMPG.

For the TSL methylation assay, TSL was dissolved in acetonitrile and then deposited in the appropriate wells of a 96-well reaction plate. The plate was dried under a vacuum for 10 minutes to remove the organic solvent. The diluted recombinant protein was then added to the plate and placed on a shaker at room temperature and 625 rpm for 5 minutes. DCMB dissolved in water was added to wells requiring DCMB, and an equal volume of water was added to the remaining wells as a vehicle control. The reaction was initiated by adding SAM at a final concentration of 100 μM. The final TSL concentration was 50 μM, the final DCMB concentration was 100 μM, and the final protein concentration was 0.07 mg/ml. The plate was again placed on a plate shaker, sealed with a silicon plate mat, and then incubated at 37°C for 30 minutes. For IC_{50} determination, METTL7A was incubated with 50 μM TSL and DCMB was added at 0.001, 0.01, 0.1, 0.5, 1.0, 10, 50, and 100 μM final concentration. In vitro assays were performed as microassays to conserve protein, and final reaction volumes were 30 μl unless otherwise specified.

After 30 minutes, the reaction was quenched with 5× the reaction volume with ice-cold ethyl acetate containing 5 μM 7α-thiomethylspironolactone-d7 deuterated internal standard (TMSL-D7). During the quench step, each sample was mixed with ethyl acetate by gentle pipetting up and down. The plate was then immediately frozen at −80°C for 12 minutes. After 12 minutes, the aqueous layer was frozen, and the liquid organic top layer was transferred to a new plate. The transferred samples were dried with gentle heat and nitrogen gas flow (Biotage, Charlotte, NC) followed by reconstitution with 50:50 acetonitrile:water containing 0.2% acetic acid. Samples were analyzed with a Waters Xevo TQS mass spectrometer paired with a Waters ACQUITY LC using a 2.1 × 50-mm Waters 1.7 μm C18 column and 0.2% acetic acid in water and 0.2% acetic acid in acetonitrile as solvents A and B, respectively. Consistent elution of TMSL and TMSL-D7 was achieved with an isocratic gradient held at a 50:50 ratio of solvent A to solvent B. Flow rate was constant at 0.4 ml/min. The transitions used to monitor for methyl metabolite 7α-thiomethylspironolactone (TMSL) and IS TMSL-D7 were 389.223 > 341.308 and 396 > 347.05, respectively, and TSL methylation was reported as the peak area ratio (PAR) of TMSL/TMSL-D7.

For captopril methylation assay, captopril dissolved in water was added to 96-well plate wells containing diluted active or boiled protein, prepared with DMPG as described above. A no-enzyme control incubation was prepared by replacing the protein-containing portion of the components with reaction buffer. DCMB dissolved in water, or water as a vehicle control, was added to the appropriate wells. The final protein concentration was 0.07 mg/ml; for wells including DCMB, the final DCMB concentration was 100 μM. The plate was placed on a shaker for 2 minutes at 625 rpm at room temperature, and the reaction was initiated by the addition of SAM to a final concentration of 100 μM. After initiating the reaction, the plate was mixed on the shaker, sealed with a silicon plate mat, and incubated at 37°C for 25 minutes. The reaction was quenched by adding 15% zinc sulfate (w/v) at one-eighth the reaction volume. The quenched solution was incubated on ice for 10 minutes before a solution of saturated barium hydroxide containing the d3-*S*-methyl captopril internal standard was added at a 1:1 v/v with zinc sulfate. The plate was mixed at 625 rpm for 2 minutes and was then incubated on ice for another 10 minutes. The 96-well plate was centrifuged at 4500 × *g* for 15 minutes to pellet all precipitated proteins and salts. The supernatant was transferred to a new 96-well plate, and NaOH was added to a final concentration of 125 mM. Finally, maleimide was added to the reaction to a final concentration of 500 mM. Maleimide reacts with unmethylated captopril to remove excess captopril and avoids complications in mass spec analysis. The plate

was sealed with a silicon plate mat, wrapped in foil, and incubated at room temperature for 1 hour. The plate was centrifuged again to precipitate any salts that had formed during the alkylation reaction, and the supernatant was transferred to a new 96-well plate and was analyzed by liquid chromatography tandem mass spectrometry (LC-MS/MS). LC-MS/MS conditions for monitoring captopril methylation were similar to those described previously by Maldonato et al. (2021). Captopril methylation was reported as the peak area ratio of Me-captopril/D3-Me-captopril subtracted from the average peak area ratio determined for the no-enzyme control group (the background).

In Vitro Michaelis-Menten Kinetics Using Recombinant METTL7A and METTL7B. Purified N-GST-METTL7A, or N-GST-METTL7B, was diluted into a DMPG-containing buffer, and TSL was deposited into the wells of a 96-well plate as described above.

For single time point experiments with increasing concentrations of SAM, TSL was added to a final concentration of 250 μM, and SAM was added at 1, 5, 10, 25, 50, 100, 250, and 1000 μM to initiate the reaction.

For the *S*-adenosyl-homocysteine (SAH) and SAM single time point activity assay matrix, TSL was added to a final concentration of 250 μM; SAH was added at 0, 5, 10, 50, and 100 μM; and SAM was added at 1, 5, 10, 25, 50, 100, 250, and 1000 μM to initiate the reaction.

For the TSL single time point activity assay with increasing concentrations of TSL, TSL was added to a final concentration of 1, 5, 10, 25, 50, 100, 250, and 1000 μM. SAM was added to a final concentration of 100 μM to initiate the reaction.

All reactions were incubated for 30 minutes at 37°C before quenching with ethyl acetate containing TMSL-D7. The reactions were quenched, processed, and analyzed similar to the procedure described above.

Substrate Screening. Potential substrates were screened for methylation using the Promega MTase-Glo Methyltransferase Assay Kit. Purified N-GST-METTL7A was diluted into a DMPG-containing buffer similar to the procedure described above. The substrate screening assay was performed in a 96-well plate at a final protein concentration of 0.07 mg/ml. Each probe substrate (1 mM final concentration) was added to the diluted enzyme. Samples were preequilibrated with shaking at 625 rpm for 5 minutes at room temperature, and the reactions were initiated by adding SAM (100 μM). The plate was sealed with a silicon plate mat and incubated at 37°C for 1 hour. Enzymatic activity was quenched by adding DCMB to a final concentration of 100 μM. A volume of 20 μl from each well in the enzyme reaction plate was transferred to a new well in a white-walled 96-well flat bottom plate, and then the plate was processed according to the manufacturer's protocol. Luminescence was recorded from each well using a Synergy HTX Multimode Reader (BioTek, Winooski, VT). All compounds were tested in triplicate with boiled and active N-GST-METTL7A, and relative turnover was determined by subtracting the response of boiled N-GST-METTL7A from active N-GST-METTL7A for each compound. The resulting difference for a no-substrate control was then subtracted from all of the active minus boiled differences that were determined for each compound using the following equation:

$$(\bar{X}(active,\ substrate) - \bar{X}(boiled,\ substrate)) - (\bar{X}(active,\ no\ substrate) - \bar{X}(boiled,\ no\ substrate)) \quad (1)$$

We noticed a significantly high background signal when using the Promega MTase-Glo Methyltransferase Assay Kit, which is likely due to the presence of a thiol compound in the developing kit that is readily methylated by METTL7A or METTL7B. It is necessary to be cautious in designing controls, quenching the reactions, and interpreting data.

Silencing METTL7A and METTL7B Genes in HepG2 Cells. HepG2 cells (Ref: HB-8065; American Type Culture Collection, Manassas VA) were cultured in Eagle's minimum essential media (EMEM) with 10% fetal bovine serum, 0.1% v/v penicillin-streptomycin and were seeded into 12-well tissue culture plates at 200,000 cells per well ($n = 3$). Cells were reverse transfected with Lipofectamine 3000 and siRNA following the manufacturer's protocol for gene knockdown. The final concentration of small interfering RNA (siRNA) per treatment was 10 nM, and the final concentration of lipofectamine 3000 reagent was 2 μl/ml. Cells were reverse transfected with siRNA targeting *METTL7A*, *METTL7B*, *METTL7A*, and *METTL7B* (combo), or scramble nonspecific siRNA (Ref: METTL7A/EHU153411, METTL7/EHU008171, Scramble/SIC001; Sigma-Aldrich). Cells were incubated with siRNA for 48 hours, washed with warm DPBS, and treated with serum-free EMEM containing TMT substrates (125 μM TSL or 500 μM captopril) in the presence or absence of 20 μM DCMB. Cells were incubated with TMT substrates for 24 hours, after which the media were collected and analyzed for methylated metabolites by LC-MS/MS. The LC-MS/MS analysis of captopril and TSL was conducted as described above. The results were normalized to the media collected from negative control scramble siRNA-treated cells. The knockdown efficiency analysis was conducted as described by Maldonato et al. (2021) using proprietary TaqMan FAM reporter primers for *METTL7A*, *METTL7B*, and the housekeeping gene *GUSB*.

Overexpression of METTL7A and METTL7B in HeLa Cells. HeLa cells (Ref: CCL-2; American Type Culture Collection) were cultured in EMEM with 10% fetal bovine serum, 0.1% v/v penicillin-streptomycin and were seeded into 6-well tissue culture plates at 500,000 cells per well ($n = 3$). The cells were reverse transfected using Lipofectamine 3000 and P3000 reagent along with different pCMV expression vectors following the manufacturer's protocol. The final concentration of pCMV plasmid expression vector per treatment was 1250 ng/ml, the final concentration of Lipofectamine 3000 reagent was 1.5 μl/ml, and the final concentration of P3000 reagent was 1 μl/ml. Cells were incubated with media containing Lipofectamine reagents and either a METTL7A (Ref: RC202601; OriGene), METTL7B (Ref: RC203838; OriGene), or empty control (Ref: PS100001; OriGene) expression vector for 36 hours. After 36 hours, the cell media were removed, the cells washed with warm DPBS, and the media replaced with serum-free EMEM containing 125 μM TSL ± 20 μM DCMB. Cells were incubated with TMT substrate for 24 hours before the media were collected and analyzed for methylated metabolites by LC-MS/MS as described above.

Protein overexpression was confirmed by western blot analysis. After incubation with the expression vector for 36 hours, cells were harvested by scraping each well with 1 ml of DPBS. Cells were then transferred to a 1.5-ml Eppendorf tube and pelleted by centrifuging for 5 minutes at 750 × *g*, 4°C. The DPBS was removed and the cells from each treatment were lysed in 150 μl of RIPA buffer containing 1× halt protease inhibitor cocktail. The lysis was performed by resuspending cells in lysis buffer and pipetting up and down 20 times. The cell lysates were analyzed for protein concentration using the bicinchoninic acid (BCA) method, and 5.5 μg of protein from each cell lysate was loaded onto a protein SDS-PAGE gel. Protein separation by gel electrophoresis and subsequent western blot analysis were performed as described above. The primary antibody incubation lasted overnight with anti-β-actin (Ref: 4970S, Lot: 18; Cell Signaling) and anti-FLAG Tag (Ref: 14793S, Lot: 5; Cell Signaling) primary antibodies. Each antibody was diluted 1:500.

Identification of METTL7A and METTL7B in Human Liver Microsomes. Pooled 50-donor human liver microsomes (Ref: HMMCPL, Lot: PL050F-B, 16 females and 34 males; Fisher Scientific) and pooled 50-donor human liver cytosol (Ref: HMMCPL, Lot: PL028-J, 16 females and 30 males; Fisher Scientific) were protein normalized, and 40 μg of protein from each subcellular fraction was loaded onto a NuPAGE 4 to 12%, Bis-Tris protein gel. Protein separation by gel electrophoresis, and subsequent western blot analysis was performed as described above. Two western blots were developed, one stained with an anti-METTL7B (Invitrogen, Carlsbad, CA, Ref: PA5-58478, Lot: XC3518324A) and the other with anti-METTL7A primary antibody (Ref: TA346478, Lot: Qa2850; OriGene). These antibodies were diluted 1:1000 and 3:1000, respectively.

Analysis of DCMB Inhibition of TMT Activity in Liver Subcellular Fractions. Fifty-donor pooled HLM and human liver cytosol were diluted to 1 mg/ml in KPi reaction buffer (50 mM KPi pH 7.0, 20% glycerol, 150 mM NaCl, 10 mM CHAPS). Captopril was added to a final concentration of 5 mM, DCMB was added to a final concentration of 100 μM, and SAM was added to a final concentration of 100 μM to initiate the reaction. The mixtures were incubated for 45 minutes at 37°C. After incubations, all samples were processed and then analyzed by LC-MS/MS using the same sample prep and LC-MS/MS method as described above in the section titled *In Vitro 7α-Thiospironolactone and Captopril Methylation Using Recombinant METTL7A and METTL7B*.

Quantification of METTL7A and METTL7B Protein Levels in Individual Donor Human Liver Microsomes. Microsomes were prepared by thawing individual donor liver samples (10 females and nine males; Supplemental Table 1) on ice in homogenization buffer (50 mM KPi pH 7.4, 250 mM sucrose, 1 mM EDTA, and 1× Halt protease inhibitor cocktail). The thawed tissue was transferred to a sterile petri dish on ice, and a razor blade was used to remove fibrotic tissue. Next, the tissues samples were placed in a 55-ml Dounce homogenizer and were homogenized using four to six passes with a powered Teflon pestle. The homogenate was transferred to a centrifuge tube and was

centrifuged at 8000 × *g* for 30 minutes at 4°C to pellet all intact cells, nuclei, and mitochondria. The supernatant was then transferred to a fresh tube and was centrifuged at 100,000 × *g* for 60 minutes at 4°C. The supernatant containing cytosolic fraction was removed, and the pellet containing the microsomal fraction was resuspended in 2 ml of homogenization buffer via Dounce homogenization and was then aliquoted and stored at −80°C until future use.

For the quantitative proteomic analysis of METTL7A and METTL7B protein levels in individual donor HLMs, protein samples were normalized to 2 mg/ml with homogenization buffer. HLM samples 30 μl of 2 mg/ml were combined with an equal volume of ammonium bicarbonate 100 mM and 10 μl of DTT (250 mM). The samples were then incubated at 37°C for 30 minutes. The samples were allowed to cool back to room temperature followed by the addition of 10 μl of iodoacetamide (IAA: 500 mM iodoacetamide in 50 mM ammonium bicarbonate) to each sample. Each sample was then vortexed and incubated for 30 minutes at room temperature in the dark. One milliliter of crash solution (methanol:chloroform:water, 5:1:4) was added to the samples and centrifuged for 5 minutes at 16,000 × *g* and 4°C. A protein pellet appeared as a disc suspended between the immiscible methanol/water and chloroform layers. Both layers were carefully aspirated, and then the protein was allowed to air dry for 10 minutes. Methanol (0.5 ml) was added to the pellet. Samples were centrifuged for 5 minutes at 8000 × *g* and 4°C, the methanol was aspirated, and the pellet was allowed to air dry for 30 minutes, followed by the addition of 20 μl of trypsin dissolved in 50mM ammonium bicarbonate at 1:80 trypsin:protein ratio (w/w). The protein pellet was digested by the trypsin for 16 hours while incubating at 37°C and shaking at 300 rpm. After digestion, 20 μl of LC/MS buffer (80% acetonitrile with 0.5% formic acid that contains the relative heavy peptides) was added to each sample. The samples where then centrifuged for 10 minutes at 4000 × *g* and 4°C. the supernatant was transferred and analyzed by LC-MS/MS.

A UPLC-MS/MS SCIEX Triple Quadrupole 6500 system (Framingham, WA) coupled to an ACQUITY UPLC system (Waters Technologies, Milford, MA) was used for proteomic analysis, and 5 μl of each sample was injected onto the column (ACQUITY UPLC CSH 1.7 μm, C18; 100 × 2.1 mm; Waters, Milford, MA). A gradient method (0.3 ml/min) with mobile phase A consisting of 0.1% formic acid in water and mobile phase B consisting of 0.1% formic acid in acetonitrile was used for peptide separation.

Two surrogate peptides obtained from Thermo Fisher Scientific (Waltham, MA) were chosen separately for METTL7A and METTL7B. The relevant transitions for each peptide are shown in Supplemental Table 2. Analyst 1.6 software (SCIEX) was used for peak integration and data analysis. PeakView 2.0 was applied for checking the quality of peaks and initial method development. Chromatographic integration and peak area analysis were performed by using Skyline 20.0.1.31 (University of Washington, Seattle, WA).

Determination of Thiol Methylation Activity across HLMs from Individual Donors. Individual liver donor microsomes diluted to 0.25 mg/ml in KPi reaction buffer (50 mM KPi pH 7.0, 20% glycerol, 150 mM NaCl, 10 mM CHAPS) were incubated with 250 μM TSL and 100 μM SAM for 30 minutes at 37°C. For the small cohort of individual donor HLMs that were incubated ± DCMB, the final TSL, DCMB, and SAM concentrations were all 100 μM. The reaction quench and downstream determination of TSL methylation were performed by LC-MS/MS as described above.

Data Analysis. Unless noted otherwise, all experiments were conducted in triplicate and all data reported as the mean ± standard deviation. Statistical significance was determined by a two-tailed unpaired student *t*-test with a threshold *P* value of 0.05. Kinetic parameters K_m (Michaelis constant) for TSL and SAM, K_i (inhibitor constant) for SAH, and IC_{50} (half-maximal inhibitory concentration) for DCMB values were calculated using GraphPad Prism version 9.4.1 for Windows (GraphPad Software, La Jolla, CA). A two-tailed Spearman's nonparametric correlation was computed to assess the relationship between two variables with a threshold *P* value of 0.05.

Results

Sequence Similarity and Structural Homology between METTL7A and METTL7B. METTL7A and METTL7B are both 244 residues long and have a molecular weight of 28 kDa, similar to prior literature regarding TMT activity (Weisiger and Jakoby, 1979). Both isoforms share 75% sequence homology and 60% sequence identity, as determined by basic local alignment search tool (BLAST) analysis (Altschul et al., 1990) (Supplemental Fig. 1). Homology models of METTL7A and METTL7B produced by AlphaFold (Jumper et al., 2021; Varadi et al., 2022) indicate high structural similarity (Fig. 1).

Expression and Purification of His-GST-METTL7A. Consistent with the previous expression of METTL7B (Maldonato et al., 2021), we inserted the METTL7A gene sequence into a pET21 expression plasmid and expressed the protein in *E. coli*. The pET21 expression vector adds a unique tag to the *N* terminus of the inserted ORF, a 10× histidine-tag (His) followed by a glutathione-*S*-transferase (GST) tag (Fig. 2.). The N-terminal GST tag is essential to solubilize METTL7A from bacterial membrane. The recombinant protein 10×His-GST-METTL7A (N-GST-METTL7A) has a molecular weight of 57.6 kDa. We confirmed the successful purification of N-GST-METTL7A with a visible protein band at ∼58 kDa by SDS-PAGE Coomassie stain (Fig. 2). A band at ∼58 kDa is also visible on a western blot using an anti-METTL7A and anti-GST-antibody; it is not visible using an anti-METTL7B-antibody (Fig. 2). The purity of recombinant METTL7A was comparable to the purity we previously achieved for recombinant METTL7B. The lower molecular weight bands that were identified as a nonfunctional GST tag portion of N-GST-METTL7B also co-purified with N-GST-METTL7A. We suspect that the HRV-(AP)5 linker-sequence between GST and METTL7A or 7B introduced a feature that leads to the formation of this N-terminal tag portion of this protein construct during the process of bacterial protein expression. There is no concern that the nonspecific proteins observed in the purified protein eluent are involved in TMT activity, as we have demonstrated with a nonfunctional D98A mutant METTL7B that there is no TMT activity in purification eluent or bacterial lysate without a functional, expressed thiol methyltransferase (Maldonato et al., 2021).

Validation of N-GST-METTL7A *S*-Methyltransferase Activity. Purified N-GST-METTL7A methylated captopril and TSL (Fig. 3) in a time- and protein-dependent fashion. Like N-GST-METTL7B, purified N-GST-METTL7A required preincubation with 1,2-dimyristoyl-sn-glycero-3-PG (DMPG) liposomes for activity (Supplemental Fig. 2).

Inhibition of METTL7A by DCMB. DCMB potently inhibits N-GST-METTL7A but not N-GST-METTL7B (Fig. 3). An IC_{50} of 1.17 μM was determined for DCMB and METTL7A using TSL as a substrate (Fig. 3). There is virtually no 7α-thiomethylspironolactone (TMSL) observed in the inactivated boil controls (Supplemental Fig. 3), and because

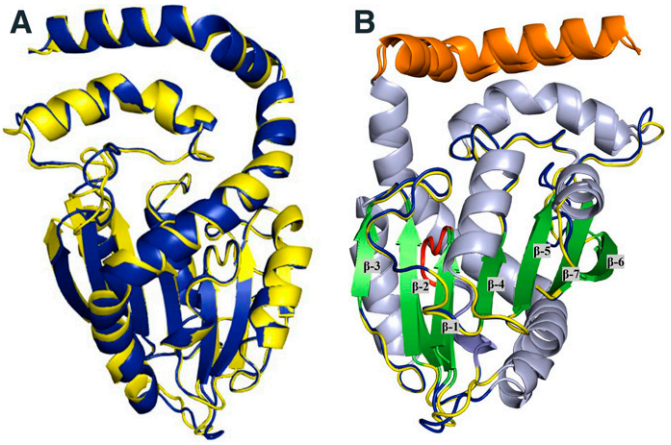

Fig. 1. AlphaFold homology models of METTL7A (TMT1A) (yellow) and METTL7B (TMT1B) (blue) aligned with PyMOL alignment function (A). AlphaFold homology models of METTL7A (TMT1A) (yellow) and METTL7B (TMT1B) (blue) aligned and oriented to visualize secondary structural features (B), with hydrophobic *N*-terminus in orange, GXGXG sequence in red, beta sheets in green and labeled β-1 through β-7 by order along the sequence, and alpha helices in light blue.

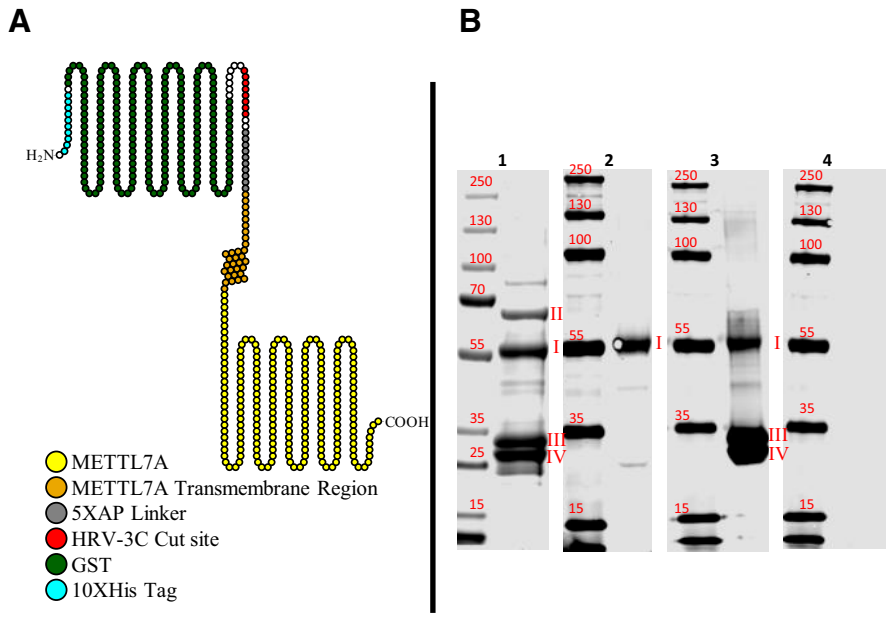

Fig. 2. Cartoon representation of *N*-GST-METTL7A (*N*-GST-TMT1A) with features highlighted and identified in the legend (A); figure produced with Protter (Omasits et al., 2014). SDS-PAGE Coomassie stain (B.1), anti-METTL7A (anti-TMT1A) western blot (B.2), anti-GST western blot (B.3), and anti-METTL7B (anti-TMT1B) western blot (B.4) of purified *N*-GST-METTL7A (*N*-GST-TMT1A). Labeled bands are *N*-GST-METTL7A (*N*-GST-TMT1A) (I), a contaminant chaperone protein (II), and GST devoid of METTL7A (TMT1A) (III, IV).

of this we deemed TSL a suitable probe substrate for further METTL7 characterization experiments.

Competitive Inhibition of N-GST-METTL7A by *S*-Adenosyl-Homocysteine. We determined the K_m for the methyl-donating cofactor SAM by measuring the formation of TMSL by LC-MS/MS (Fig. 4). The SAM activity curve followed Michaelis-Menten kinetics with a K_m for SAM at 53.73 μM. Analysis of the METTL7A homology model generated by AlphaFold indicated that this protein is a class I small-molecule methyltransferase (Supplemental Fig. 4). Class I methyltransferases have a conserved binding site with a high affinity for SAM and the demethylated cofactor *S*-adenosyl-homocysteine (SAH) (Schubert et al., 2003). As expected with a class I small-molecule methyltransferase, SAH inhibited TSL methylation in a concentration-dependent manner and exhibited a competitive mechanism of inhibition with respect to SAM (Fig. 4), with a K_i of 53.86 μM. This value is similar to the K_i that we previously determined for METTL7B (Maldonato et al., 2021). We measured all kinetic parameters under linear conditions for incubation time and protein concentration (Supplemental Fig. 5). For SAM and SAH kinetic analysis, a saturating amount of TSL was added for these assays to be under conditions of no substrate depletion.

Kinetic Analysis of *N*-GST-METTL7A and *N*-GST METTL7B *S*-Methylation of TSL. We determined the K_m value for TSL by measuring the formation of TMSL for both N-GST-METTL7A and N-GST-METTL7B by LC-MS/MS (Fig. 4). The TSL activity curves for each enzyme followed Michaelis-Menten kinetics. The K_m values for TSL methylation by METTL7A and METTL7B were 39.41 and 32.50 μM, respectively. The K_m for TSL methylation by recombinant METTL7B by LC-MS/MS, an orthogonal approach to our previous analysis, was similar to what we have previously reported for METTL7B (Maldonato et al., 2021).

Substrate Specificity of N-GST-METTL7A. Substrates for class I small-molecule methyltransferases were screened for N-GST-METTL7A methylation with the Promega MTase-Glo kit. In previous screens with this assay kit, METTL7B activity was normalized to dopamine, a compound that showed no activity. Normalization was necessary because METTL7B produced a high response in the kit in absence of a substrate

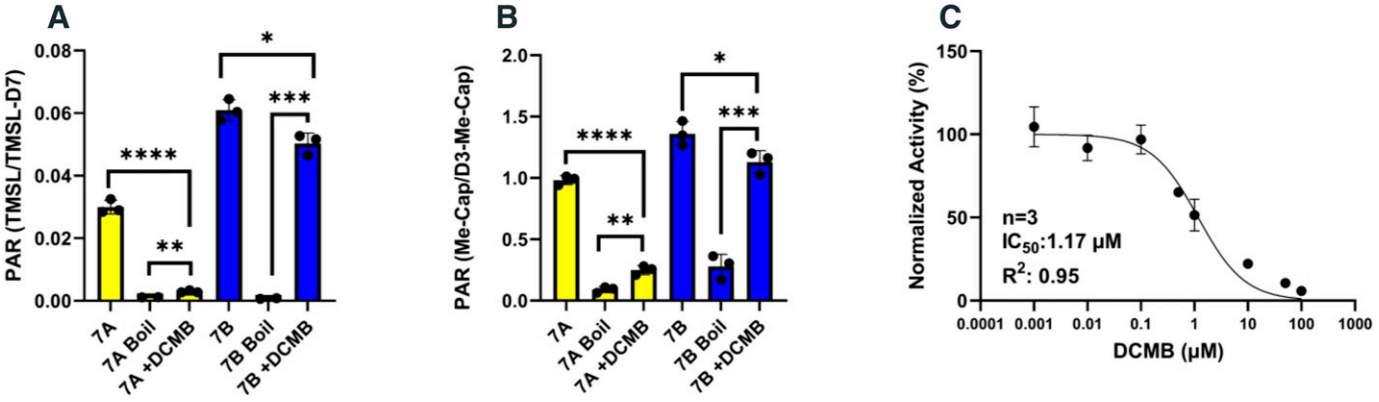

Fig. 3. Methylation of TSL by purified recombinant *N*-GST-METTL7A (*N*-GST-TMT1A) and *N*-GST-METTL7B (*N*-GST-TMT1B) ± DCMB (A) or captopril (B). IC_{50} for the inhibition of purified recombinant *N*-GST-METTL7A (*N*-GST-TMT1A) by DCMB was determined by single time point activity assays with increasing concentrations of DCMB (C). Data (n = 3) are reported as the mean ± S.D. ****$P < 0.0001$; ***$P < 0.001$; **$P < 0.01$.

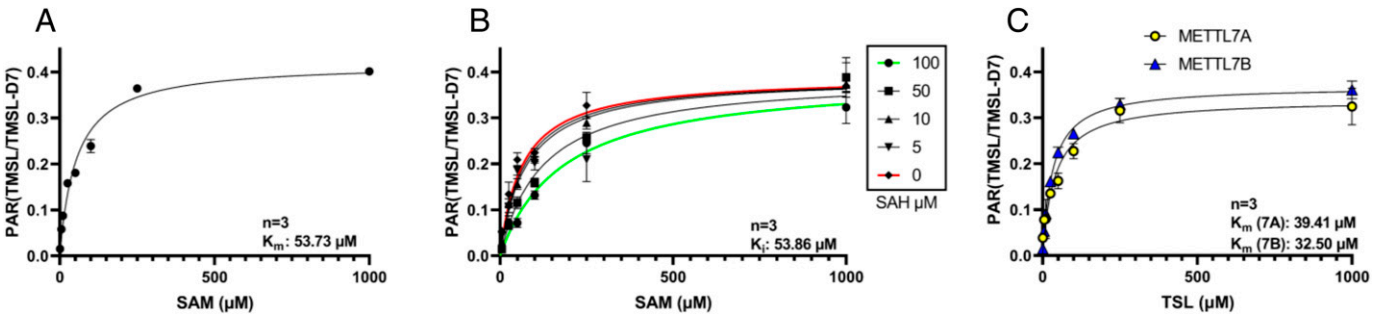

Fig. 4. TSL methylation by N-GST-METTL7A (*N*-GST-TMT1A) at various concentrations of SAM in absence (A) or presence of increasing concentrations of SAH (B); and single time point kinetics profiles of N-GST-METTL7A (*N*-GST-TMT1A) or N-GST-METTL7B (*N*-GST-TMT1B) with increasing concentrations of TSL (C). Data ($n = 3$) are reported as the mean ± S.D.

compared with a boiled enzyme control. METTL7A, incubated without a substrate, also demonstrated a high response compared with the boiled enzyme. Adding DCMB as a quench step at the end of incubation significantly reduced the baseline signal (Supplemental Fig. 6). This observation indicates that METTL7A and METTL7B catalyze the methylation of a compound in the reagents supplied with the kit. As such, it became standard practice to include DCMB in the quench step to prevent further METTL7A activity during downstream signal development steps.

Potential substrates were screened at concentrations at least three times higher than their literature-reported K_m values to ensure the detection of methylated metabolites (Weisiger and Jakoby, 1979; Rivett and Roth, 1982; Drummer et al., 1983; Hiemke and Ghraf, 1983; Keith et al., 1984; Keith et al., 1985; Grunewald et al., 1989). METTL7A preferentially methylated exogenous thiol-containing compounds and did not methylate the endogenous thiols tested, cysteine and glutathione (Fig. 5). METTL7A did not methylate compounds that are known O- and N-methyltransferase substrates. Mertansine, a thiol-containing microtubule inhibitor, was significantly methylated. We also tested *S*-methyl mertansine as a negative control, and the response was not significantly above baseline. We assume that mertansine can only be methylated on the thiol moiety. Since *S*-methyl mertansine has no available site for further methylation, we used *S*-methyl mertansine activity level in the kit as a nonsubstrate baseline control for screening other potential substrates with the Promega MTase-Glo assay.

Modulating METTL7A and METTL7B Gene Expression in HepG2 Cells and Its Effect on Thiol Methylation Activity. HepG2 cells were treated with scrambled negative control siRNA, METTL7A-specific small interfering RNA (siRNA), METTL7B-specific siRNA, or a combination of both. METTL7A-specific siRNA exclusively reduced METTL7A gene expression by 90%, whereas METTL7B-specific siRNA reduced the expression of METTL7B and METTL7A by 90% and 30%, respectively. The nonspecific reduction in METTL7A gene expression using a METTL7B-specific siRNA is likely caused by the siRNA design. The METTL7B-specific siRNA shares 60% sequence identity with a METTL7A-coding mRNA segment, potentially inducing modest suppression (Supplemental Fig. 7). The combined treatment of METTL7A- and METTL7B-specific siRNA reduced the expression of both genes by 90% (Fig. 6). After incubation with siRNA for 48 hours, cell media were replaced with media containing either TSL or captopril. The methylated metabolites for each compound were measured in the culture media by LC-MS/MS. We observed the largest decrease in TSL and captopril methylation in the combined siRNA-treated cell media compared with cells treated with control siRNA. The smallest decrease was observed in METTL7B-specific siRNA-treated cell media (Fig. 6).

Modulating METTL7A and METTL7B Protein Levels in HeLa Cells and Its Effect on Thiol Methylation Activity. HeLa cells were incubated with pCMV expression vectors encoding FLAG-tagged METTL7A, FLAG-tagged METTL7B, or an empty insert to act as a negative control. Protein expression of METTL7A or METTL7B was determined in cell lysate by protein normalized anti-FLAG western blotting. An anti-β-actin antibody was included as a costain for loading control. FLAG-tagged METTL7A and METTL7B are visible at the correct molecular weights, only in lysates of cells incubated with the appropriate expression vector (Fig. 7). No FLAG-tagged protein is visible in the empty control vector-treated cells. Cells expressing FLAG-tagged METTL7A or FLAG-tagged METTL7B had significantly increased TSL methylation compared with empty vector control-treated cells, determined by LC-MS/MS (Fig. 7). With the addition of DCMB, only METTL7A-overexpressing cells showed a significant reduction in TSL methylation compared with cells not treated with DCMB.

Subcellular Localization of METTL7A and METTL7B in Human Liver. Using 50-donor pooled HLMs, we observed bands at the molecular weight of 28 kDa in anti-METTL7A and anti-METTL7B stained western blots (Fig. 8). We observed similar bands in the pooled liver cytosolic fraction, albeit at much lower intensities.

We determined TMT activity in the 50-donor pooled microsomal or cytosolic fractions, that were protein normalized to 1 mg/ml, by measuring captopril methylation via LC-MS/MS analysis (Fig. 8). HLMs contained the highest TMT activity, whereas lowest TMT activity was observed in liver cytosol, which had 30% TMT activity compared with HLMs.

We determined the effect of DCMB on TMT activity in pooled HLMs and cytosol by adding saturating concentrations of DCMB during captopril methylation assays (Fig. 8). There was ≥70% reduction in TMT activity in HLMs and liver cytosol when incubated with DCMB. In a similar inhibition experiment, we screened individual donor HLMs for TMT activity ± DCMB using TSL instead of captopril as the probe substrate (Fig. 8). Saturating concentrations of DCMB added during TSL methylation assays reduced each individual donor HLM's TMT activity by >80%.

Quantifying of METTL7A and METTL7B Protein Levels in HLMs and Correlation with *S*-Methylation Activity. We quantified METTL7A and METTL7B protein levels in 19 adult single-donor HLMs by LC-MS/MS quantitative proteomics (Fig. 9). METTL7A protein levels are, on average, 3-fold higher than METTL7B levels. We also determined TSL methylation activity in the same donor HLMs (Fig. 9). There was an 8-fold difference in activity among all donors.

We computed a nonparametric Spearman's correlation to assess the relationship between METTL7A and METTL7B protein levels. The Spearman correlation coefficient was 0.89, and the P value was <0.0001 (Fig. 9). This indicates a positive correlation between METTL7A and METTL7B. We also calculated a Spearman correlation coefficient to

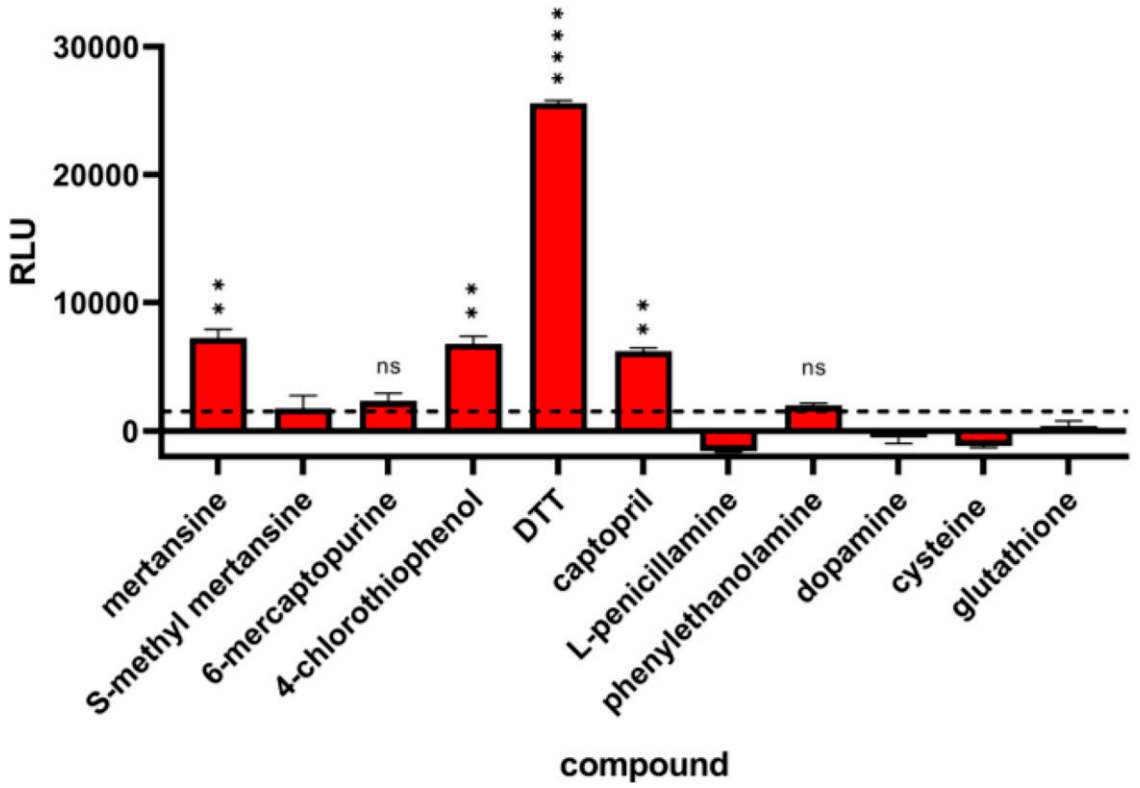

Fig. 5. Semiquantitative screening of select small molecule methyltransferase probe substrates. Known methyltransferase probe substrates were incubated at saturating concentrations for 1 hour with *N*-GST-METTL7A (*N*-GST-TMT1A). Formation of SAH (indication of methyl transfer) was converted/directly linked to luminescence and measured via the Promega MTase-Glo kit. Enzyme activity was determined after normalizing to compound-specific and general assay background signal. All data ($n = 3$) are presented as the mean ± S.D. Significance was determined using unpaired two-tailed *t*-test comparing the baseline subtracted response of each compound with that of S-methyl mertansine as a baseline (dotted line). $^{****}P < 0.0001$; $^{***}P < 0.001$; $^{**}P < 0.01$.

assess the relationship between relative TSL methylation activity and the combined protein levels of METTL7A and METTL7B. The Spearman correlation coefficient for this analysis was 0.87, and the *P* value was <0.0001 (Fig. 9). This indicates a positive correlation between METTL7A and METTL7B protein levels and relative TMT activity across individual HLMs.

Discussion

The key finding in this investigation is that METTL7A is a thiol methyltransferase and along with METTL7B, both enzymes account for most of *S*-thiol methylation activity in HLMs. We will refer to METTL7A and METTL7B as thiol methyltransferase 1A (TMT1A) and thiol methyltransferase 1B (TMT1B), respectively, for the rest of the discussion and use *TMT1A* (https://www.ncbi.nlm.nih.gov/gene/25840) and *TMT1B* (https://www.ncbi.nlm.nih.gov/gene/196410) when referring to the genes as agreed upon with the HUGO Gene Nomenclature Committee. TMT1A can selectively methylate exogenous alkyl and phenolic thiols and is inhibited by DCMB, the historic TMT inhibitor with an IC_{50} of 1.17 μM, which is within the range of the previously determined IC_{50} of 0.45 μM for TMT activity in HLMs (Glauser et al.,

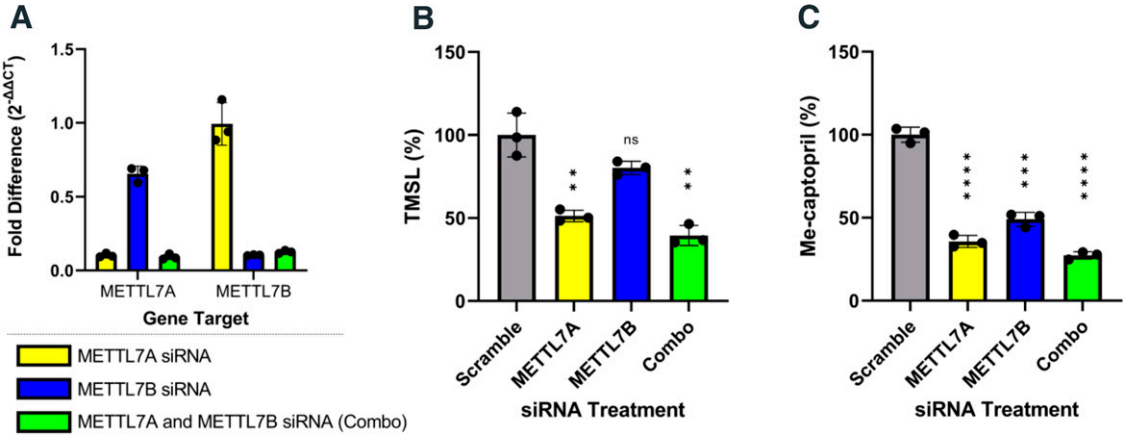

Fig. 6. Knockdown of *METTL7A* (*TMT1A*) and *METTL7B* (*TMT1B*) in HepG2 cells. Reverse-transcription polymerase chain reaction (RT-PCR) data measuring fold difference of *METTL7A* (*TMT1A*) or *METTL7B* (*TMT1B*) expression after 48-hour siRNA treatment with *METTL7A* (*TMT1A*)- and/or *METTL7B* (*TMT1B*)-targeting siRNA (A). Percent TMSL (B) and S-methyl captopril (C) formed in cell media. All data ($n = 3$) are presented as the mean ± S.D. Significance was determined using an unpaired two-tailed *t* test. $^{****}P < 0.0001$; $^{***}P < 0.001$; $^{**}P < 0.01$.

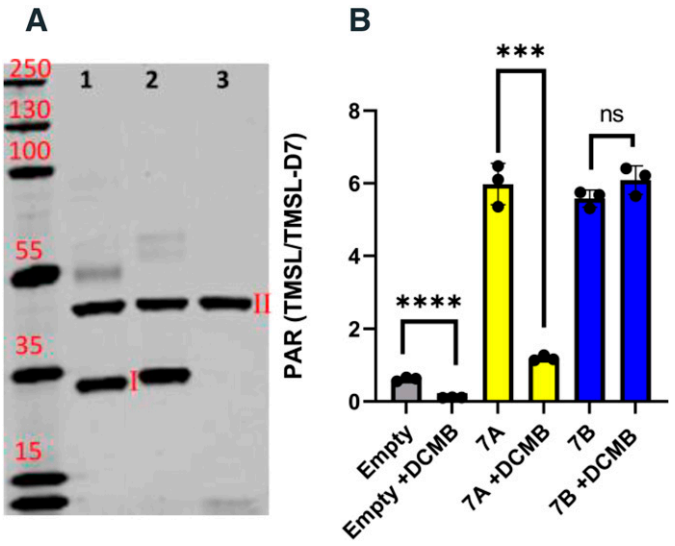

Fig. 7. Overexpression of METTL7A (TMT1A) and METTL7B (TMT1B) in HeLa cells. Anti-flag and anti-β-actin western blots verify the overexpression of flag-tagged proteins in METTL7A (TMT1A) (A.1) and METTL7B (TMT1B) (A.2), which show a band at I, compared with cells treated with empty vector control (A.3). Labeled bands are flag-tagged METTL7A (TMT1A) and flag-tagged METTL7B (TMT1B) (I) and β-actin (II). Formation of TMSL in HeLa cells overexpressing METTL7A (TMT1A) or METTL7B (TMT1B) after a 24-hour incubation with TSL ± DCMB (B). All data (n = 3) are presented as the mean ± S.D. Significance was determined using unpaired two-tailed t test. $^{****}P < 0.0001$; $^{***}P < 0.001$; $^{**}P < 0.01$.

1993). Therefore, although TMT1B is a thiol methyltransferase, it cannot entirely account for TMT activity because DCMB has no effect on its activity. TMT1A shares 60% sequence identity with TMT1B and has a similar substrate specificity, yet only TMT1A is potently inhibited by DCMB. Further work is required to determine the structural features in TMT1A that confer DCMB selectivity compared with TMT1B.

Recombinant TMT1A transfers a methyl group to several exogenous thiol-containing compounds, including DTT, mertansine, captopril, and 6-chlorothiophenol, in a general methyltransferase substrate screening assay. Similar to prior reports for TMT activity, TMT1A did not methylate endogenous thiols including cysteine and glutathione or other small molecules specific for N- and O-methyl transferases (Weisiger and Jakoby, 1979), although other endogenous thiols may be substrates.

TMT1A behaves like a class I small molecule methyltransferase, determined by a series of kinetic experiments. TMT1A utilizes SAM as the methyl donor and methylates TSL following classic Michaelis-Menten kinetics (Fig. 4). It is competitively inhibited by SAH, as evidenced by higher SAM concentrations diminishing SAH inhibition. The Michaelis constant (K_m) for SAM and TSL is 53.73 μM and 39.41 μM, respectively, within the range of the values 43 μM and 27 μM previously reported in the literature (Weinshilboum et al., 1979; Keith et al., 1984). In addition, we compared the kinetic curves of TSL methylation by TMT1A and TMT1B and established that both recombinant enzymes have similar K_m values for TSL. The K_m value for TMT1B mediated methylation of TSL, reported by LC-MS/MS, was 32.50 μM, close to the value determined in our previous study, which instead used the Promega MTase-Glo Methyltransferase Assay to report on the methylation of TSL.

TMT1A and *TMT1B* gene–silencing experiments in HepG2 cells caused a significant decrease in *S*-methylation activity, whereas overexpression of *TMT1A* and *TMT1B* in HeLa cells significantly increased TMT activity. Only HeLa cells overexpressing TMT1A had reduced TMT activity with DCMB addition, confirming that the TMT1A's specificity for exogenous alkyl and phenolic thiols is not influenced by the in vitro expression or incubation systems that were used in these studies.

TMT activity is described in the literature as most abundant in liver microsomes (Weisiger and Jakoby, 1980; Weisiger et al., 1980; Drummer et al., 1983), and an RNA sequencing analysis reported that like TMT, *TMT1A,* and *TMT1B* expression levels are highest in the human liver (Karlsson et al., 2021) compared with other tissues. By western blot analysis, we determined that TMT1A and TMT1B are present in human liver and are associated with the microsomal fraction. We also confirmed that TMT activity is highest in the microsomal fraction and lowest in the cytosol consistent with previous reports (Bremer and Greenberg, 1961; Borchardt and Cheng, 1978; Weisiger and Jakoby, 1979; Pacifici et al., 1991).

Saturating concentrations of DCMB added to a TMT activity assay performed in HLMs results in ≥70% decrease in TMT activity toward captopril methylation and >80% decrease in activity toward TSL methylation. Since TMT1A is potently inhibited by DCMB whereas TMT1B is not, TMT1A is responsible for most of TMT activity in HLMs whereas the remaining activity with saturating concentrations of DCMB can be attributed to TMT1B. Finally, we measured the protein levels of TMT1A and TMT1B by quantitative proteomics. TMT1A protein levels are, on average, 3-fold greater than TMT1B, but the two proteins are highly correlated. TMT activity was determined for each donor and correlated well with the sum of TMT1A and TMT1B protein levels, as observed in Fig. 9.

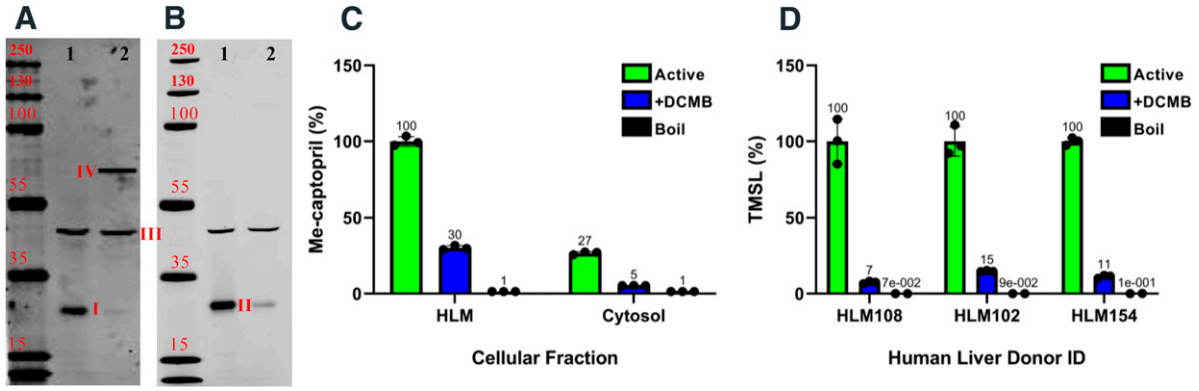

Fig. 8. Anti-METTL7A (anti-TMT1A) (A) and anti-METTL7B (anti-TMT1B) (B) western blots of human liver microsomes (1) and cytosol (2). Labeled bands are METTL7A (TMT1A) (I), METTL7B (TMT1B) (II), and β-actin (III), and the band at IV is an unknown protein that reacts with anti-METTL7A (anti-TMT1A) antibody in the cytosolic fraction. Relative formation of S-methyl-captopril in pooled human liver microsomes and cytosol ± DCMB (C). Relative formation of TMSL in individual liver donor microsomes ± DCMB (D). All treatments performed in triplicate (n = 3) except for (D) boil controls, which were performed in duplicate (n = 2). All data are presented as the mean ± S.D.

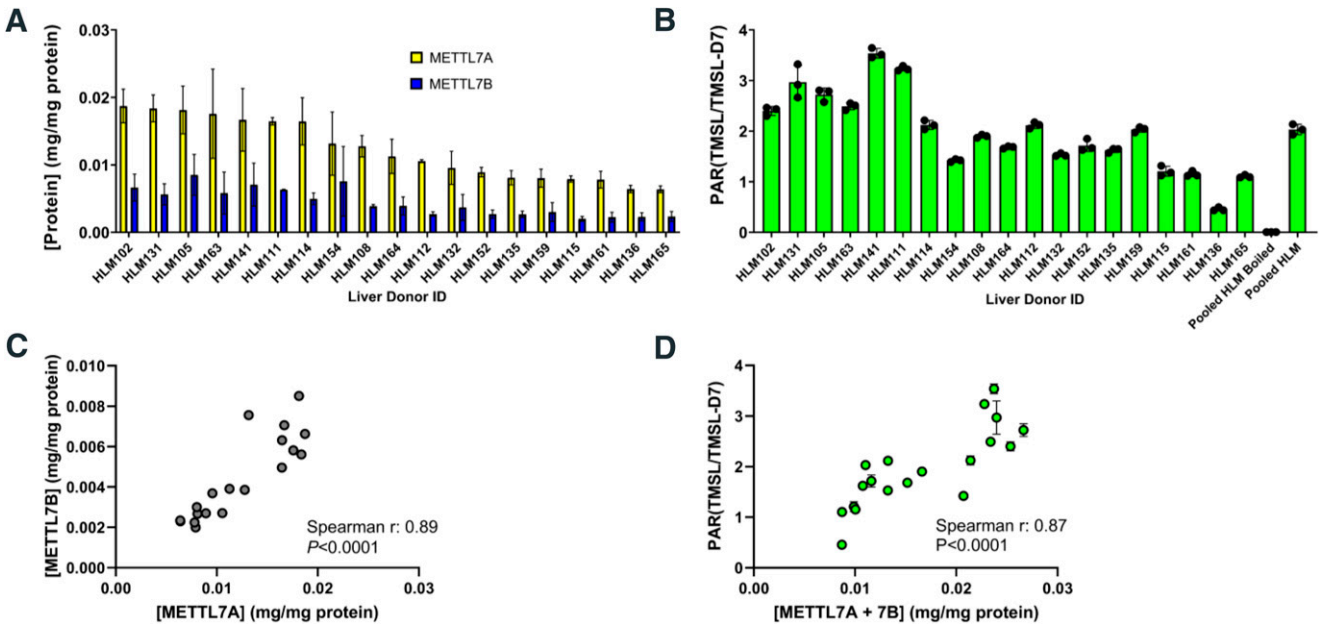

Fig. 9. METTL7A (TMT1A) and METTL7B (TMT1B) protein levels measured in individual donor HLMs using quantitative proteomics; protein levels of METTL7A (TMT1A) and METTL7B (TMT1B) are reported normalized to total protein per digestion (A). Methyltransferase activity, reported as peak area ratio (PAR), of single-donor HLMs incubated with TSL, and SAM (B) compared with commercially available 50-donor pooled HLMs. METTL7A (TMT1A) and METTL7B (TMT1B) protein correlation (C). TMT activity correlation with METTL7A (TMT1A) and METTL7B (TMT1B) protein levels (D). Data are presented as the mean ± S.D.

The high TMT1A and TMT1B protein levels in the liver compared with other tissue and their association with the endoplasmic reticulum parallel other drug-metabolizing enzymes like cytochrome P450 enzymes. Other class I small molecule methyltransferases such as catechol-O-methyltransferase (COMT), phenylethanolamine N-methyltransferase (PNMT), and nicotinamide N-methyltransferase (NNMT) have very limited examples of exogenous substrates but clear examples of endogenous ones—dopamine, noradrenaline, and nicotinamide, respectively (Aksoy et al., 1994; Drinkwater et al., 2009; Júlio-Costa et al., 2013). In this regard, it is reasonable to consider TMT1A and TMT1B as drug metabolizing enzymes, but they could also have an endogenous role such as the methylation of hydrogen sulfide or other endogenous thiol-containing biomolecules. We have previously reported that TMT1B methylates hydrogen sulfide (Maldonato et al., 2021), and preliminary data from our laboratory suggests that TMT1A also methylates hydrogen sulfide (data not shown).

Although the endogenous function of TMT1A and TMT1B remains unknown, their dysregulation is continually reported in different diseases, especially cancer. In one large-cohort multicancer multiomics study, higher *TMT1A* expression was determined to have the most favorable survival across cancers compared with other METTLs (Campeanu et al., 2021). *TMT1B*, antithetically, is significantly upregulated across most cancers (Jiang et al., 2021). TMT1B regulates the epithelial-mesenchymal transition of thyroid cancer cells in the presence of TGF-β, an important regulator of cancer immunosuppression (Ye et al., 2019; Chen et al., 2021; Xiong et al., 2021), and in multiple cell lines, TMT1B promotes G1 to S phase transition in cancer cells (Liu et al., 2020; Li et al., 2021). *TMT1B* overexpression is attributed to proliferation and tumorigenesis, which suggests an oncogenic role in cancer progression. Conversely, the consistent lower expression of *TMT1A* across cancers would suggest a tumor-suppressing role. Although the nature of TMT1A and TMT1B's involvement in cancers is not well understood, the high level of dysregulation of *TMT1A* and *TMT1B* might impact the metabolism of thiol-containing chemotherapeutics by cancer cells.

Our results are inconsistent with one report suggesting that TMT1A and TMT1B are capable of RNA methylation (Wang et al., 2022), but our results align with a recent report that TMT1A and TMT1B are involved in the *S*-methylation of histone deacetylase inhibitor romidepsin (Robey et al., 2023). Although we cannot rule out that TMT1A or TMT1B may have RNA-methylating functions and further work is needed to confirm this function, the microsomal association of these enzymes strongly suggests a role in small-molecule methyl transfer.

In summary, our findings support the hypothesis that TMT1A and TMT1B account for the majority of microsomal TMT activity. Future work will focus on identifying endogenous thiol-containing substrates for TMT1A and TMT1B and examining their role in tumorigenesis.

Acknowledgments

The authors wish to thank the late Scott Edgar for his advice and contribution to mass spectrometry assay development.

Data Availability

The authors declare that all of the data supporting the findings of this study are available within the paper and its Supplemental Material.

Authorship Contributions

Participated in research design: Russell, Chau, Shi, Maldonato, Totah.
Conducted experiments: Russell, Chau, Shi, Levasseur, Maldonato.
Contributed new reagents or analytic tools: Russell, Chau, Shi.
Performed data analysis: Russell, Chau, Shi, Totah.
Wrote or contributed to the writing of the manuscript: Russell, Chau, Shi, Maldonato, Totah.

References

Agusti G, Bourgeois S, Cartiser N, Fessi H, Le Borgne M, and Lomberget T (2013) A safe and practical method for the preparation of 7α-thioether and thioester derivatives of spironolactone. *Steroids* **78**:102–107.

Aksoy S, Szumlanski CL, and Weinshilboum RM (1994) Human liver nicotinamide N-methyltransferase. cDNA cloning, expression, and biochemical characterization. *J Biol Chem* **269**: 14835–14840.

Altschul SF, Gish W, Miller W, Myers EW, and Lipman DJ (1990) Basic local alignment search tool. *J Mol Biol* **215**:403–410.

Bargh JD, Isidro-Llobet A, Parker JS, and Spring DR (2019) Cleavable linkers in antibody-drug conjugates. *Chem Soc Rev* **48**:4361–4374.

Borchardt RT and Cheng CF (1978) Purification and characterization of rat liver microsomal thiol methyltransferase. *Biochim Biophys Acta* **522**:340–353.

Bremer J and Greenberg DM (1961) Enzymic methylation of foreign sulfhydryl compounds. *Biochim Biophys Acta* **46**:217–224 DOI: 10.1016/0006-3002(61)90746-6.

Campeanu IJ, Jiang Y, Liu L, Pilecki M, Najor A, Cobani E, Manning M, Zhang XM, and Yang Z-Q (2021) Multi-omics integration of methyltransferase-like protein family reveals clinical outcomes and functional signatures in human cancer. *Sci Rep* **11**:14784.

Chen X, Li C, Li Y, Wu S, Liu W, Lin T, Li M, Weng Y, Lin W, and Qiu S (2021) Characterization of METTL7B to evaluate TME and predict prognosis by integrative analysis of multi-omics data in glioma. *Front Mol Biosci* **8**:727481.

Drinkwater N, Gee CL, Puri M, Criscione KR, McLeish MJ, Grunewald GL, and Martin JL (2009) Molecular recognition of physiological substrate noradrenaline by the adrenaline-synthesizing enzyme PNMT and factors influencing its methyltransferase activity. *Biochem J* **422**:463–471.

Drummer OH, Miach P, and Jarrott B (1983) S-methylation of captopril. Demonstration of captopril thiol methyltransferase activity in human erythrocytes and enzyme distribution in rat tissues. *Biochem Pharmacol* **32**:1557–1562.

Erickson HK, Widdison WC, Mayo MF, Whiteman K, Audette C, Wilhelm SD, and Singh R (2010) Tumor delivery and in vivo processing of disulfide-linked and thioether-linked antibody-maytansinoid conjugates. *Bioconjug Chem* **21**:84–92.

Glauser TA, Saks E, Vasova VM, and Weinshilboum RM (1993) Human liver microsomal thiol methyltransferase: inhibition by arylalkylamines. *Xenobiotica* **23**:657–669.

Grunewald GL, Ye Q, Sall DJ, Criscione KR, and Wise B (1989) Conformational and steric aspects of phenylethanolamine and phenylethylamine analogues as substrates or inhibitors of phenylethanolamine N-methyltransferase. *Mol Pharmacol* **35**:93–97.

Hiemke C and Ghraf R (1983) Distribution and properties of thiol S-methyltransferase in rat brain. *J Neurochem* **40**:592–594.

Jiang Z, Yin W, Zhu H, Tan J, Guo Y, Xin Z, Zhou Q, Cao Y, Wu Z, Kuang Y, et al. (2021) METTL7B is a novel prognostic biomarker of lower-grade glioma based on pan-cancer analysis. *Cancer Cell Int* **21**:383.

Júlio-Costa A, Antunes AM, Lopes-Silva JB, Moreira BC, Vianna GS, Wood G, Carvalho MR, and Haase VG (2013) Count on dopamine: influences of COMT polymorphisms on numerical cognition. *Front Psychol* **4**:531.

Jumper J, Evans R, Pritzel A, Green T, Figurnov M, Ronneberger O, Tunyasuvunakool K, Bates R, Žídek A, Potapenko A, et al. (2021) Highly accurate protein structure prediction with AlphaFold. *Nature* **596**:583–589.

Karlsson M, Zhang C, Méar L, Zhong W, Digre A, Katona B, Sjöstedt E, Butler L, Odeberg J, Dusart P, et al. (2021) A single-cell type transcriptomics map of human tissues. *Sci Adv* **7**:eabh2169.

Kazui M, Hagihara K, Izumi T, Ikeda T, and Kurihara A (2014) Hepatic microsomal thiol methyltransferase is involved in stereoselective methylation of pharmacologically active metabolite of prasugrel. *Drug Metab Dispos* **42**:1138–1145.

Keith RA, Jardine I, Kerremans A, and Weinshilboum RM (1984) Human erythrocyte membrane thiol methyltransferase. S-methylation of captopril, N-acetylcysteine, and 7 alpha-thio-spirolactone. *Drug Metab Dispos* **12**:717–724.

Keith RA, Otterness DM, Kerremans AL, and Weinshilboum RM (1985) S-Methylation of D- and L-penicillamine by human erythrocyte membrane thiol methyltransferase. *Drug Metab Dispos* **13**:669–676.

Krynetski E and Evans WE (2003) Drug methylation in cancer therapy: lessons from the TPMT polymorphism. *Oncogene* **22**:7403–7413.

Lennard L (2014) Implementation of TPMT testing. *Br J Clin Pharmacol* **77**:704–714.

Li W, Xu S, Peng N, Zhang Z, He H, Chen R, Chen D, Fan J, and Wang X (2021) Downregulation of METTL7B inhibits proliferation of human clear cell renal cancer cells *in vivo* and *in vitro*. *Front Oncol* **11**:634542.

Liu C, Chen Z, Zhong K, Li L, Zhu W, Chen X, and Zhong D (2015) Human liver cytochrome P450 enzymes and microsomal thiol methyltransferase are involved in the stereoselective formation and methylation of the pharmacologically active metabolite of clopidogrel. *Drug Metab Dispos* **43**:1632–1641.

Liu D, Li W, Zhong F, Yin J, Zhou W, Li S, Sun X, Xu J, Li G, Wen Y, et al. (2020) METTL7B is required for cancer cell proliferation and tumorigenesis in non-small cell lung cancer. *Front Pharmacol* **11**:178.

Lopus M, Oroudjev E, Wilson L, Wilhelm S, Widdison W, Chari R, and Jordan MA (2010) Maytansine and cellular metabolites of antibody-maytansinoid conjugates strongly suppress microtubule dynamics by binding to microtubules. *Mol Cancer Ther* **9**:2689–2699.

Maldonato BJ, Russell DA, and Totah RA (2021) Human METTL7B is an alkyl thiol methyltransferase that metabolizes hydrogen sulfide and captopril. *Sci Rep* **11**:4857.

Maw HH, Zeng X, Campbell S, Taub ME, and Teitelbaum AM (2018) *N*-methylation of BI 187004 by thiol *S*-methyltransferase. *Drug Metab Dispos* **46**:770–778.

Obach RS, Prakash C, and Kamel AM (2012) Reduction and methylation of ziprasidone by glutathione, aldehyde oxidase, and thiol S-methyltransferase in humans: an in vitro study. *Xenobiotica* **42**:1049–1057.

Omasits U, Ahrens CH, Müller S, and Wollscheid B (2014) Protter: interactive protein feature visualization and integration with experimental proteomic data. *Bioinformatics* **30**:884–886.

Overdiek HW and Merkus FW (1987) The metabolism and biopharmaceutics of spironolactone in man. *Rev Drug Metab Drug Interact* **5**:273–302.

Pacifici GM, Santerini S, Giuliani L, and Rane A (1991) Thiol methyltransferase in humans: development and tissue distribution. *Dev Pharmacol Ther* **17**:8–15.

Rivett AJ and Roth JA (1982) Kinetic studies on the O-methylation of dopamine by human brain membrane-bound catechol O-methyltransferase. *Biochemistry* **21**:1740–1742.

Robey RW, Fitzsimmons CM, Guiblet WM, Frye WJE, Dalmasy JMG, Wang L, Russell DA, Huff LM, Perciaccante AJ, Ali-Rahmani F, et al. (2023) The methyltransferases METTL7A and METTL7B confer resistance to thiol-based histone deacetylase inhibitors. *bioRxiv*:2022.2010.2007.511310.

Savi P, Zachayus JL, Delesque-Touchard N, Labouret C, Hervé C, Uzabiaga MF, Pereillo JM, Culouscou JM, Bono F, Ferrara P, et al. (2006) The active metabolite of clopidogrel disrupts P2Y12 receptor oligomers and partitions them out of lipid rafts. *Proc Natl Acad Sci USA* **103**:11069–11074.

Schubert HL, Blumenthal RM, and Cheng X (2003) Many paths to methyltransfer: a chronicle of convergence. *Trends Biochem Sci* **28**:329–335.

Taplin S, Vashisht K, Walles M, Calise D, Kluwe W, Bouchard P, and Johnson R (2018) Hepatotoxicity with antibody maytansinoid conjugates: a review of preclinical and clinical findings. *J Appl Toxicol* **38**:600–615.

Varadi M, Anyango S, Deshpande M, Nair S, Natassia C, Yordanova G, Yuan D, Stroe O, Wood G, Laydon A, et al. (2022) AlphaFold Protein Structure Database: massively expanding the structural coverage of protein-sequence space with high-accuracy models. *Nucleic Acids Res* **50** (D1):D439–D444.

Wang Z, He J, Bach DH, Huang YH, Li Z, Liu H, Lin P, and Yang J (2022) Induction of m^6A methylation in adipocyte exosomal lncRNAs mediates myeloma drug resistance. *J Exp Clin Cancer Res* **41**:4.

Weinshilboum RM and Sladek SL (1980) Mercaptopurine pharmacogenetics: monogenic inheritance of erythrocyte thiopurine methyltransferase activity. *Am J Hum Genet* **32**:651–662.

Weinshilboum RM, Sladek S, and Klumpp S (1979) Human erythrocyte thiol methyltransferase: radiochemical microassay and biochemical properties. *Clin Chim Acta* **97**:59–71.

Weisiger RA and Jakoby WB (1979) Thiol S-methyltransferase from rat liver. *Arch Biochem Biophys* **196**:631–637.

Weisiger RA and Jakoby WB (1980) S-methylation: thiol S-methyltransferase, in *Enzymatic Basis of Detoxication*, 1st ed (Jakoby WB, ed) **vol 2**, Elsevier.

Weisiger RA, Pinkus LM, and Jakoby WB (1980) Thiol S-methyltransferase: suggested role in detoxication of intestinal hydrogen sulfide. *Biochem Pharmacol* **29**:2885–2887.

Wusk B, Kullak-Ublick GA, Rammert C, von Eckardstein A, Fried M, and Rentsch KM (2004) Thiopurine S-methyltransferase polymorphisms: efficient screening method for patients considering taking thiopurine drugs. *Eur J Clin Pharmacol* **60**:5–10.

Xiong Y, Li M, Bai J, Sheng Y, and Zhang Y (2021) High level of METTL7B indicates poor prognosis of patients and is related to immunity in glioma. *Front Oncol* **11**:650534.

Yates CR, Krynetski EY, Loennechen T, Fessing MY, Tai HL, Pui CH, Relling MV, and Evans WE (1997) Molecular diagnosis of thiopurine S-methyltransferase deficiency: genetic basis for azathioprine and mercaptopurine intolerance. *Ann Intern Med* **126**:608–614.

Ye D, Jiang Y, Sun Y, Li Y, Cai Y, Wang Q, Wang O, Chen E, and Zhang X (2019) METTL7B promotes migration and invasion in thyroid cancer through epithelial-mesenchymal transition. *J Mol Endocrinol* **63**:51–61.

Zehmer JK, Bartz R, Liu P, and Anderson RG (2008) Identification of a novel N-terminal hydrophobic sequence that targets proteins to lipid droplets. *J Cell Sci* **121**:1852–1860.

Address correspondence to: Dr. Rheem A. Totah, Department of Medicinal Chemistry, Health Sciences Building H-172, University of Washington, 1959 NE Pacific St, PO Box 357610, Seattle, WA 98195. E-mail: rtotah@uw.edu